論文 / 著書情報
Article / Book Information

Title	Enhancement of Thin McKibben Muscle Durability Under Repetitive Actuation in a Bent State
Authors	Ryota Kobayashi, Hiroyuki Nabae, Zebing Mao, Gen Endo, Koichi Suzumori
Citation	IEEE Robotics and Automation Letters, Volume 9, Issue 11, Page 9685 - 9692
Pub. date	2024, 9
DOI	https://doi.org/10.1109/LRA.2024.3455890
Creative Commons	Information is in the article.

Enhancement of Thin McKibben Muscle Durability Under Repetitive Actuation in a Bent State

Ryota Kobayashi, Hiroyuki Nabae, *Member, IEEE*, Zebing Mao, *Member, IEEE*, Gen Endo, *Member, IEEE*, and Koichi Suzumori, *Senior Member, IEEE*

***Abstract*—The McKibben muscle can produce a high force-to-mass ratio, beneficial for various applications in the soft mechatronics field. The thin McKibben muscle, which has a small diameter, has the advantage of a high force-to-mass ratio and sufficient flexibility for use in a bent state. This flexibility permits the realization of flexible mechatronics. However, the thin McKibben muscle is easily broken in a bent state while it is very durable in a straight state. Over repetitive operations, the fibers within the sleeve gradually shift, causing the rubber tube inside to protrude and ultimately leading to cracking. This study investigates improvements in the durability of artificial muscles using adhesives to prevent this fiber-to-fiber misalignment. The durability test showed that the adhesive could provide a durability of up to 10,000-times greater than that of a normal thin artificial muscle in the maximum case. Using the thin McKibben muscle with the proposed method, tensegrity modules were fabricated. The durability test revealed a 500-fold increase under an applied pressure of 0.5 MPa. Furthermore, the durability of the adhesive-applied artificial muscles was also confirmed to be enhanced during the dynamic movements of a soft tensegrity robot that throws a ball with 0.7 MPa.**

***Index Terms*—Thin McKibben muscle, soft sensors and actuators, durable, soft tensegrity robot.**

I. Introduction

SOFT robots inspired by living organisms and their muscles have advantages such as the ability to flexibly adapt to their environment and safely and cooperatively work alongside humans [1]. Soft actuators, flexible sensors, and flexible materials have been studied extensively in recent years for the development of soft robots, and soft mechatronics, which integrates soft actuators and robots, has been developed. Soft actuators in soft mechatronics are a major determinant of robot performance. McKibben muscles are a practical type of pneumatic soft actuators with a high force-to-weight ratio [2]. This actuator comprises a rubber tube and a sleeve and generates axial contraction of approximately 20% in the inflated state. This property is beneficial for various applications in robotics [3], such as robotic arms [4], [5] and hopping robots [6].

Received 11 May 2024; accepted 28 August 2024. Date of publication 6 September 2024; date of current version 27 September 2024. This article was recommended for publication by Associate Editor N. Gravish and Editor Y.-L. Park upon evaluation of the reviewers' comments. This work was supported by JSPS International Joint Research Program (JRPs) . under Grant JPJSJRP20221502. *(Corresponding author: Ryota Kobayashi.)*

Ryota Kobayashi, Hiroyuki Nabae, Gen Endo, and Koichi Suzumori are with the Department of Mechanical Engineering, Tokyo Institute of Technology, Tokyo 152-8550, Japan (e-mail: kobayashi.r.at@m.titech.ac.jp).

Zebing Mao is with the Faculty of Engineering, Yamaguchi University, Yamaguchi 755-8611, Japan.

This letter has supplementary downloadable material available at https://doi.org/10.1109/LRA.2024.3455890, provided by the authors.

Digital Object Identifier 10.1109/LRA.2024.3455890

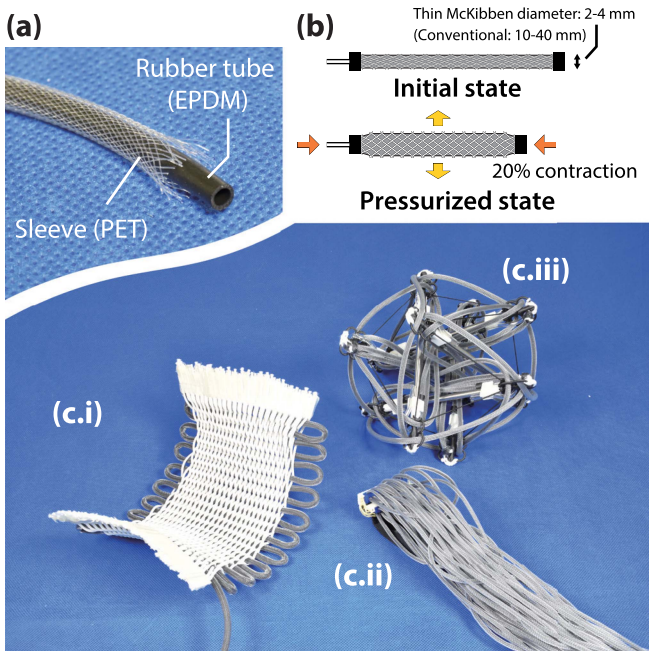

Fig. 1. (a) Composition of thin McKibben muscles. (b) Driving mechanism of thin McKibben muscles. (c) Flexible robot using artificial muscles in bent states. (c-i) Cloth-like mechanism [11]. (c-ii) Muscle textile for a soft power support suit [12]. (c-iii) Soft tensegrity module [15].

Thin McKibben muscles [7] (Fig. 1(a)) have a smaller diameter ranging from 2 to 5 mm, while conventional ones have diameters ranging from 10 to over 40 mm (Fig. 1(b)). Due to the small size of thin McKibben muscles, myriad small soft robots and devices have been developed, including a walking robot [8], soft exoskeleton glove [9], thin and long robotic strap manipulator [10]. Moreover, the small diameter of thin McKibben muscles achieves high flexibility during operation and allows their use in a bent state, which is challenging for conventional McKibben muscles because of their large diameter.

In the field of soft mechatronics, robots have been developed utilizing the properties of thin McKibben muscles that can be driven even in a bent state. One example is an active textile that can be operated flexibly by incorporating artificial muscles as fibers [11], [12] (Fig. 1(c.i) and (c.ii)). Fig. 1(c.i) and 1(c.ii) show structures in which artificial muscles are woven into fibers and other artificial muscles, respectively. These weaves can be achieved due to the flexibility of the thin McKibben muscles. When weaving the fibers and artificial muscles, a cloth-like structure can be realized (Fig. 1(c.i)), and this type of active

textile is utilized for wearable assistive devices [13], [14]. In addition, when weaving artificial muscles together, contractions of more than 25% can be achieved, and this has been applied to realize soft power support suits [12]. Another example is our previously developed thin-McKibben-muscle-driven soft tensegrity modules [15], [16], [17] (Fig. 1(c.iii)). The tensegrity modules achieved larger and more diverse movements compared to tensegrity robots employing other actuators, such as electromagnetic motors [18], [19], [20] or traditional McKibben muscles [21].

The critical factor affecting the realization of the aforementioned robots is the use of artificial muscles in a state of rapid flexion. However, muscle durability decreases significantly under bending conditions, withstanding only several tens repetitive operations under extreme conditions [11], [12], [15], while actuators arranged in a linear configuration exhibit high durability, permitting over 1 million repetitive operations. Durability is a common issue for soft actuators [22] and improving it is desirable.

Therefore, this study proposes an approach to enhance the durability of thin artificial muscles during repetitive movements in bending states. The most important factor affecting the durability of artificial muscles in flexion is the misalignment of fibers in the sleeve. Our proposed method is to add adhesive-made partitions on the fibers-crossing section to prevent misalignment. Its effectiveness is verified by conducting durability tests under various conditions, and the proposed method highly improved the durability of thin artificial muscles in a bent state. Tensegrity arms are developed using normal and highly durable artificial muscles. The durability of tensegrity arm under challenging condition is verified by subjecting the thin McKibben muscles to high pressure of 0.7 MPa to generate a significant flow rate. The contribution of this letter is advancing the practical application of soft robots by improving their durability.

The remainder of this letter is organized as follows. In Section II, mechanisms of damage to thin artificial muscles in the bent states are clarified, and a new method for improving durability is proposed. Section III describes the details of the durability tests of thin artificial muscles using the proposed method. In Section IV, the application of enhanced-durability thin artificial muscles to tensegrity robots is demonstrated. Finally, the last section presents the conclusions of this study.

II. Method For Improving the Durability of Thin McKibben Muscles Used in a Bent State

A. Damage Mechanisms of Thin Artificial Muscles in Bent States After Repeated Operation

In this study, we used artificial muscles (EM40, s-muscle Co., Ltd.) to conduct our experiments. The artificial muscle is composed of a rubber tube with an outer diameter of 4 mm made of ethylene propylene diene monomer (EPDM) and a sleeve made of polyethylene terephthalate (PET) (Fig. 1(a)). According to the report from S-Muscle Co., Ltd., the artificial muscles used in this study can withstand reciprocating actuations of 1 million times at 0.3 MPa when arranged linearly.

The authors have identified failure mechanisms for artificial muscles. Here, we describe Damage mode 1 (Fig. 2(c)), which significantly affects thin artificial muscles driven in flexion. This study proposes a method to prevent actuator failure due to this mode. In Section III-B, we discuss Damage mode 2 (Fig. 5),

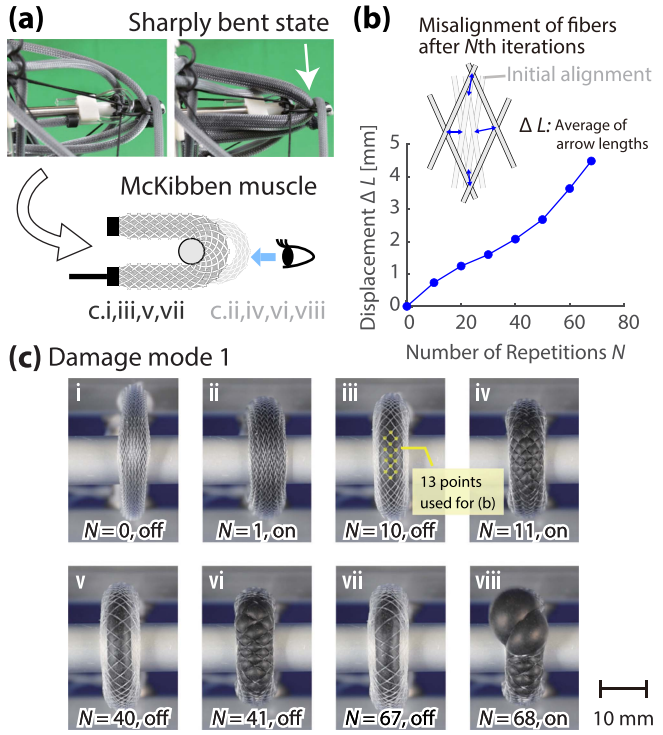

Fig. 2. (a) Appearance of the driving state of the thin McKibben muscle in a bent state. (b) Fiber-to-fiber misalignment of the sleeve of the artificial muscle during repetitive driving in a bent state. (c) Mechanism of thin pneumatic artificial muscle breakage.

a failure mode we discovered after long-cycle durability tests. In the authors' thin artificial muscle-driven tensegrity robot [15] [16] and artificial muscle weaving [23], we observe the phenomenon of artificial muscle failure at sharp bending points. Fig. 2(a) shows thin artificial muscles arranged in a sharply bent state within a tensegrity robot. To simulate this arrangement of artificial muscles within the tensegrity structure, we created a simplified reproduction using metal pipes, as shown in Fig. 2(a) (further details of the setup will be explained in Section III-B).

We observed the bent thin artificial muscles in the experiments by repeatedly actuating them every 2 s. Changes in the positions of the fibers of the sleeve can be observed in Fig. 2(c.i, iii, v, vii). Fig. 2(b) shows the variation in the displacement of the fibers at the cross-section of the sleeve when no pneumatic pressure is applied (Fig. 2(c.i, iii, v, vii)). The displacement ΔL for the Nth iteration was calculated by measuring the displacement from the initial state of multiple points at the cross-section of the artificial muscle sleeve (Fig. 2(c)), and its value is given by:

$$\Delta L(N) = \frac{1}{n}\sum_{i=1}^{n}\sqrt{(x_{i,N}-x_{i,0})^2+(y_{i,N}-y_{i,0})^2}, \quad (1)$$

where n, $x_{i,0}$ and $y_{i,0}$, and $x_{i,N}$ and $y_{i,N}$ respectively represent the number of points, the x and y coordinates of each of n points in the initial state, and the x and y coordinates of each of the n points for the Nth iteration. Here, n was set to 13 (Fig. 2(c.iii)). As shown in Fig. 2(b), the displacement was 4.5 mm in the 67th iteration, resulting in increased mesh size of the sleeve and finally causing protrusion and cracking of the rubber tube

(Fig. 2(c.viii)) in the 68th iteration. This displacement ΔL should ideally be maintained at 0 mm.

B. Prevention of Fiber Displacement in Sleeves by the Application of an Adhesive to Improve the Thin McKibben Muscle Durability

The aforementioned mechanism, described in Section. II-A, indicates that preventing the displacement of fibers in the sleeve can enhance the durability of thin artificial muscles during repetitive bending operations. A method has been proposed to fuse the crossed portion of the sleeve using a sleeve made of fusible yarn to prevent the displacement of fibers [24]. However, conventional thin artificial muscles are typically composed of non-fusible yarn, making the application of this method challenging. In addition, the requirement of a furnace for fusion complicates the processing. Therefore, we proposed a new method to prevent the displacement of fibers using adhesive (LOCTITE 401, Henkel AG & Co. KGaA) as a simple method.

As the fibers are woven, the two fibers are subjected to forces in the direction of attraction, respectively. Therefore, the misalignment of fibers can be prevented by attaching partitions, as shown in Fig. 3(a.i). We replicated this partition using an adhesive, which is applied to the cross-section where fibers intersect, as shown in Fig. 3(a.ii). After the adhesive has cured, the excess adhesive can be removed by forcing the fibers to move externally to achieve the partition shown in Fig. 3(a.i). In selecting the adhesive, two key factors were considered: the fluidity before curing and the adhesive strength after curing. A low viscosity before curing is crucial as it allows easier application of the adhesive to the sleeve without forming a membrane over the mesh. Additionally, high adhesive strength after curing is desirable to ensure the adhesive remains in place during operation. To meet these requirements, we selected LOCTITE 401, which has a low viscosity (70 to 110 mPa · s) and high shear strength (for example, 10 N/mm^2 for PVC and 9.6 N/mm^2 for polycarbonate).

In this study, we added the adhesive to the cross-section of the sleeve by rolling the sleeve on the adhesive (Fig. 3(b)). First, the adhesive was spread on a silicone rubber block (EcoFlex00-30, Smooth-On, Inc) (Fig. 3(b.i, ii)). For the block, a material that does not allow adhesives to seep into is desirable, so the silicone was used. The sleeve filled with the metal bar was rolled over the spread adhesive to apply it to the cross-section of the sleeve (Fig. 3(b.iii)). Adequate ventilation was ensured during the adhesive application process. The adhesive must be prevented from forming a membrane on the mesh of the sleeve during this process as it may compromise the stretchability of the sleeve. To prevent the sleeve from entering the mesh and forming a membrane on it, two key factors are important: the area of the mesh when applying adhesive to the sleeve and the thickness of the adhesive layer spread on the silicone block.

First, the formation of a membrane by the sleeve on the mesh can be attributed to the weak force of attraction between molecules that act to reduce the surface area of the adhesive, i.e., surface tension. By considering surface tension, the mesh area should be larger for preventing the adhesive from making a membrane on the sleeve. To achieve this, the diameter of the metal rod passing through the sleeve is adjusted to enlarge the mesh area of the sleeve. Fig. 3(c) illustrates the variables related to the sleeve's fibers. The sleeve consists of $2n$ fibers, with each fiber spirally wound. The wavelength of one fiber's spiral is denoted as L_0, as shown in Fig. 3(c). In addition, D_0 represents the initial diameter of the sleeve, D is the diameter during deformation, θ_0 is the initial knit angle, θ is the knit angle during deformation, t is the fiber diameter, and a is the length of one side of the diamond-shaped mesh. Then, the (2) expresses

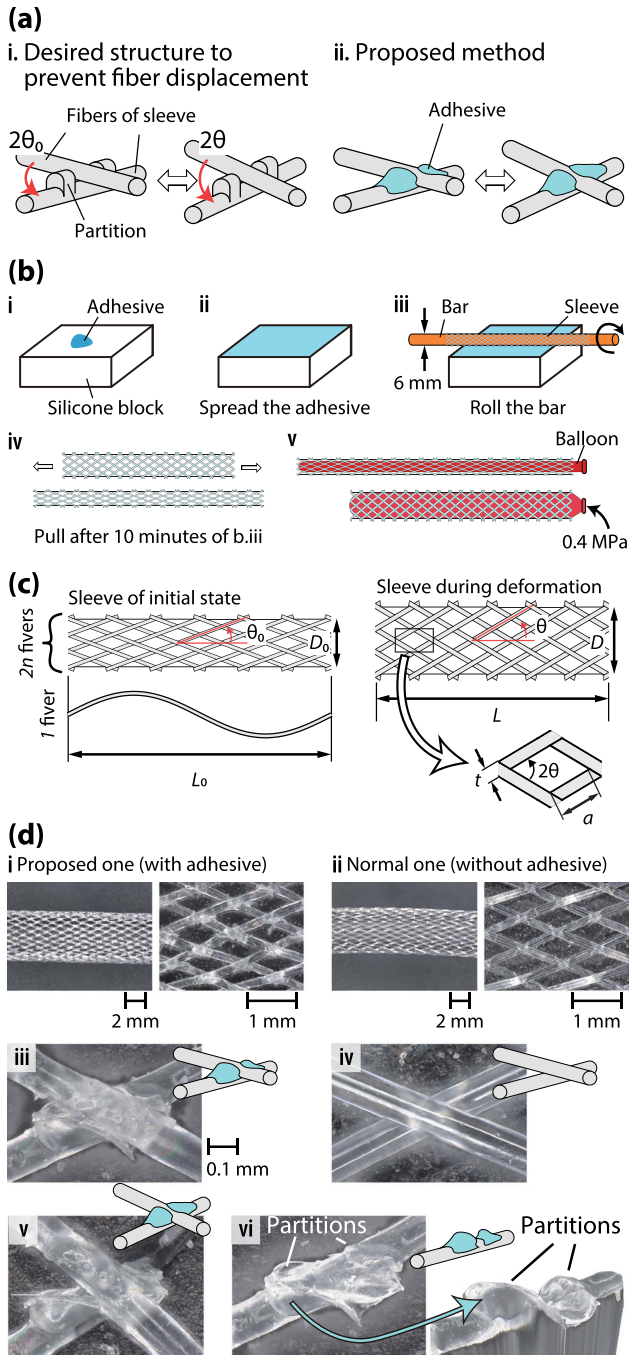

Fig. 3. Proposed method of enhancement of thin pneumatic artificial muscle durability in a bent state using adhesive. (a) Structures to prevent fiber displacement. (b) Method of application of adhesive to the sleeve. (c) Modeling of thin McKibben muscle sleeve. (d.i,ii) Surface of the sleeve of the artificial muscle. Enlargement diagram of one fiber crossing point of the artificial muscle with (d-iii) and without (d-iv) the adhesive. (d-v) Enlargement diagram of one fiber crossing point of the pressurized artificial muscle with the adhesive. (d-vi) Partitions made of the adhesive (the rightmost image was made using the focus stacking method).

the mesh area in this context.

$$S = a^2 \sin 2\theta \tag{2}$$

Furthermore, among the $2n$ fibers, n fibers have spirals in the opposite direction to the other n fibers. Consequently, there are n mesh areas within the axial distance of L_0 in the sleeve. Considering the fiber diameter, the length of one side of the mesh a is given by (3).

$$a = \frac{L}{2n\cos\theta} - \frac{t}{\sin 2\theta} \tag{3}$$

Considering that the length of one spiral revolution of a single fiber remains constant even when the sleeve undergoes deformation, the following equation can be obtained [25]:

$$\frac{L_0}{\cos\theta_0} = \frac{L}{\cos\theta}, \quad \frac{\pi D_0}{\sin\theta_0} = \frac{\pi D}{\sin\theta}. \tag{4}$$

Using (2)–(4), the mesh area can be calculated as a function that is solely dependent on the sleeve's diameter, i.e., the diameter D of the inserted metal rod. From Fig. 3(d), it can be observed that $t = 0.16$ mm, $\theta_0 = 22$ deg, $L_0/n = 1.6$ mm, and $D_0 = 4.2$ mm. With these values, it is determined that the mesh area S in (2) reaches its maximum when D is 7.9 mm. However, thicker rods increase the sleeve's braiding angle, significantly affecting muscle performance. We therefore used a 6mm rod, maintaining over 90% of the maximum area.

In addition, it is necessary to consider the layer of adhesive spread on the silicone. For a thick adhesive layer, the adhesive is applied to the metal rod. Consequently, the adhesive on the metal rod may cause the formation of a membrane on the mesh of the sleeve. Therefore, it is essential to spread the adhesive thinly enough to prevent the application of the adhesive to the metal rod. In this study, we aimed to produce a layer of adhesive with a thickness of 0.08 mm, half the diameter of the fiber. The density of the adhesive was 1.05 g/cm^3, and silicone rubber with an area of 70 mm $\times$ 40 mm was used. It was assumed that half of the adhesive adheres to the brush side when spread. In this case, it was considered that a 0.08-mm-thick adhesive layer would be formed by applying 0.47 g of adhesive, and approximately 0.5 g of adhesive was used.

Based on the measures described above, it becomes more difficult for adhesive to form a membrane on the mesh of the sleeve. The adhesive was applied by rolling the sleeve approximately five times.

The use of a 6 mm metal rod causes an increase in the knit angle of the sleeve. To rectify this, the sleeve was pulled from both sides, as indicated in Fig. 3(b.iv), after allowing the adhesive to cure for approximately 10 minutes, just long enough to prevent it from forming a membrane on the sleeve, restoring the knit angle to its normal state.

After allowing the adhesive to cure for approximately 1 h, the specified section of the sleeve, as shown in Fig. 3(a.ii), was bonded, resulting in the loss of stretchability. In this state, inserting the rubber tube into the sleeve is difficult. Therefore, a long balloon was inserted into the sleeve, and a pressure of 0.4 MPa was applied. By inflating the sleeve from the inside, the adhesive attached to the two fibers separated from one of the fibers. Instead of using a balloon, the sleeve may be pulled radially by hand to loosen it. As a result, the two fibers with applied adhesive were detached, allowing the sleeve to regain its contraction function.

A digital microscope (VHX-8000 series, Keyence Corp.) was used to investgiate the sleeve, which is shown in Fig. 3(d), and it was observed that both sleeves had a knit angle of approximately 22 deg from Fig. 3(d.i, ii). Fig. 3(d.iii) shows the fiber-to-fiber crossing of the adhesive coated artificial muscle and Fig. 3(d.iv) shows the fiber-to-fiber crossing of the normal artificial muscle. Fig. 3(d.v) shows the same area as Fig. 3(d.iii) after 0.5 MPa was applied. Fig. 3(d.vi) shows the lower fiber in Fig. 3(d.iii), and the three-dimensional shape of the sleeve surface obtained by focus stacking is shown on the right-hand side, and the partition structure was observed.

During the bonding process, approximately 20% of the sleeves failed owing to factors such as insufficient or excessive adhesive application. In the durability test of the next section, these failed sleeves were excluded, and the experiments were conducted with the remaining successfully bonded sleeves.

III. Performance Evaluation of Thin McKibben Muscles Using the Proposed Method

A. Actuation Performance of Thin McKibben Muscles Using the Proposed Method

Artificial muscles (EM40, s-muscle Co., Ltd.) are subjected to a high pressure of approximately 0.6 MPa to enhance the flexibility of the inner rubber tube initially. This improves the contraction ratio of the artificial muscles when applying normal driving pressures such as 0.3 MPa or 0.4 MPa.

Fig. 4(a) and (b) illustrate the operation of artificial muscles with adhesive and conventional artificial muscles. When a pressure of 0.5 MPa was applied in the unloaded state, both types of artificial muscles exhibited similar contraction ratios. The relationship between the pressure and contraction ratio is shown in Fig. 4(c). In addition, Fig. 4(d) and (e) depict the relationships between the pressure and contraction force and the relationship between the contraction ratio and contraction force when a pressure of 0.4 MPa was applied, respectively. In all cases (Fig. 4(c)–(e)), data were measured for five specimens, and the averages were used for plotting. In the three critical relationships shown in Fig. 4(c), (d), and (e), which represent important characteristics of artificial muscles, the artificial muscle with adhesive demonstrated a performance similar to that of the conventional artificial muscle. Fig. 4(f) shows the time response of the contraction ratio when 0.5 MPa was applied as a step input. Fig. 4(g) shows the time constant of the contraction ratio when a step pressure input is given. Fig. 4(f) and (g) were obtained by calculating the average of 5 times measurements. There are no big difference even in time response.

Furthermore, artificial muscles with adhesive has a flexibility similar to that of conventional ones. It was confirmed that the adhesive-coated-muscles could be driven in a bent state.

B. Durability of Thin McKibben Muscles Using the Proposed Method Under Repetitive Actuation in a Bent State

The ratio D/d of the diameter D of the wrapping rod to the diameter d of the artificial muscle and the angle φ of the artificial muscle are important indices that express the degree of flexion of the artificial muscle. The smaller the D/d and φ values, the more severe the bending. In addition, the pneumatic pressure may also

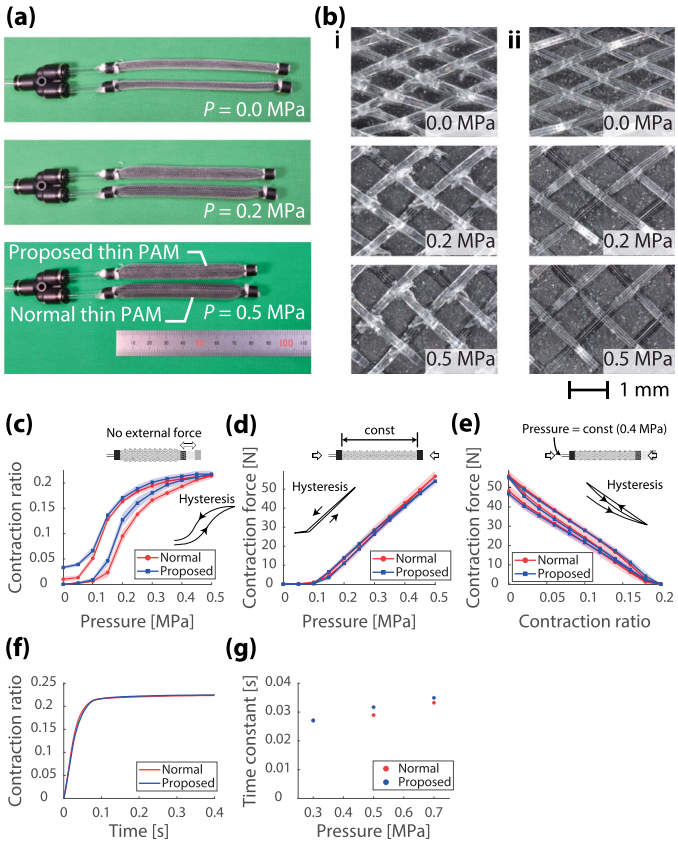

Fig. 4. (a) Contraction of normal thin McKibben muscle and thin McKibben muscle using the proposed method. (b) Surface of the sleeve. (c) Contraction ratio with respect to pressure applied to muscle. (d) Contraction force with respect to pressure applied to muscle. (e) Contraction force with respect to contraction ratio under a pressure of 0.4 MPa. (f) Time response of the contraction ratio. (g) Time constant of the contraction ratio given a step pressure input.

influence artificial muscles damage. We examined how D/d, φ, and pressure P affect the durability of artificial muscles.

The setup for the durability test is shown in Fig. 5(a). The 100 mm length of artificial muscles were used. The ends of each artificial muscle are attached to an aluminum frame using ropes, screws, and washers. The artificial muscles are arranged such that they are wound around a metal rod. Each artificial muscle is connected to a solenoid valve (025E1, KOGANEI). The compressed air from the compressor is adjusted to 0.5 MPa by a regulator, sent to the solenoid valve, and controlled by a microcontroller to drive the artificial muscles. The durability test of the artificial muscles was conducted by repeatedly applying and exhausting 0.5 MPa of compressed air in a 1-s ON, 1-s OFF cycle.

The results of the durability test are presented in Fig. 5(b)–(d). Each data point represents the average and standard error of durability tests conducted on five specimens. In addition, the durability test was conducted up to 1,000,000 cycles. A specimen that has endurerd a million cycles test is considered to have a life cycle of one million.

As shown in Fig. 5(b), the durability was examined for artificial muscles with a diameter of 4 mm and another set of artificial muscles with a diameter of 2 mm (EM20, s-muscle). The tests were conducted based on the ratio of the diameter of the metal rod around which the artificial muscle was wound to that of the artificial muscle. In this case, the angle formed by the artificial muscle φ was set to 0 deg. In Fig. 5(c), artificial muscles with a diameter of 4 mm were used, and the artificial muscle angle φ, as shown in Fig. 4(c), was set to 0 deg, 22.5 deg, 45 deg, 67.5 deg, and 90 deg. The diameter of the winding pipe was set to 10 mm. In Fig. 5(d), artificial muscles with a diameter of 4 mm were used, and the pneumatic pressure was set to 0.3, 0.5, and 0.7 MPa. The diameter of the winding pipe was set to 10 mm and the artificial muscle angle φ was set to 0 deg. In all cases (Fig. 5(b)–(d)), the blue data points represent measurements obtained using normal thin artificial muscles, while the red data points represent measurements obtained using thin artificial muscles with the proposed method.

Here, we describe Damage mode 2 of the artificial muscle. Fig. 5(e.i) shows the surface of the rubber tube of the artificial muscle after long cycles durability test, and it was confirmed that there was a scar on the rubber tube. The damage is shown in Fig. 5(e.ii) and (e.iii), where air leaks through a minute hole with a diameter of approximately 0.5 mm when a pneumatic pressure is applied. This damage mode is not due to the misalignment of the sleeve fibers. This effect was more pronounced in the case of adhesive-treated muscles. This is due to the differences in fiber surfaces as shown in Fig. 3(d)

From Fig. 5(b), it is confirmed that the proposed method is effective in all cases where D/d is less than 6. When the proposed method was used, the sleeve misalignment shown in Fig. 2(c) did not occur, and failure occurred through Damage mode 2. For D/d less than 6, normal artificial muscles experienced Damage mode 1, while proposed one experienced Damage mode 2. However, for D/d greater than 6, both cases experienced Damage mode 2. The failure occurred through Damage mode 2, resulting in worse performance when using the proposed method. In addition, artificial muscles with a diameter of 2 mm, which have thinner rubber, showed a lower life cycles due to Damage mode 2.

From Fig. 5(c), it is confirmed that the proposed method is effective when the angle formed by the artificial muscle is 67.5 deg or less. In Fig. 5, damage occurred through Damage Mode 2in all cases where the proposed method was utilized. For an artificial muscle angle of 90 deg, the four specimens of normal artificial muscles were damaged via Damage Mode 2 and only one specimen experienced damage through Damage Mode 1. In contrast, using the proposed method, all cases of 90 deg artificial muscles experienced damage through Damage Mode 2 and withstood approximately 20,000 cycles operations. One of five specimens with proposed and normal muscles each endured 1,000,000 cycles at 45 deg and 90 deg, respectively.

From Fig. 5(d), it was confirmed that the higher the pressure, the more likely the artificial muscles were to be damaged. A pressure of 0.3 MPa resulted in the failure of three adhesive-coated specimens, while the other two specimens withstood 1,000,000 cycles of durability testing. All normal artificial muscles endured 1,000,000 cycles at 0.3MPa. When 0.7 MPa was applied, all the normal artificial muscles failed via Damage Mode 1, while two specimens of the adhesive-treated muscles failed via Damage Mode 1 and three specimens failed via Damage Mode 2. This suggests that the partition structure of the adhesive-treated muscle was gradually damaged by the application of 0.7 MPa.

The results presented in Fig. 5(b)–(d) demonstrate that the proposed method can resolve the severe Damage mode 1. However, when D/d is greater than 6 (Fig. 5(b)), the artificial muscle angle φ is 90 deg (Fig. 5(c)), and the pneumatic pressure is

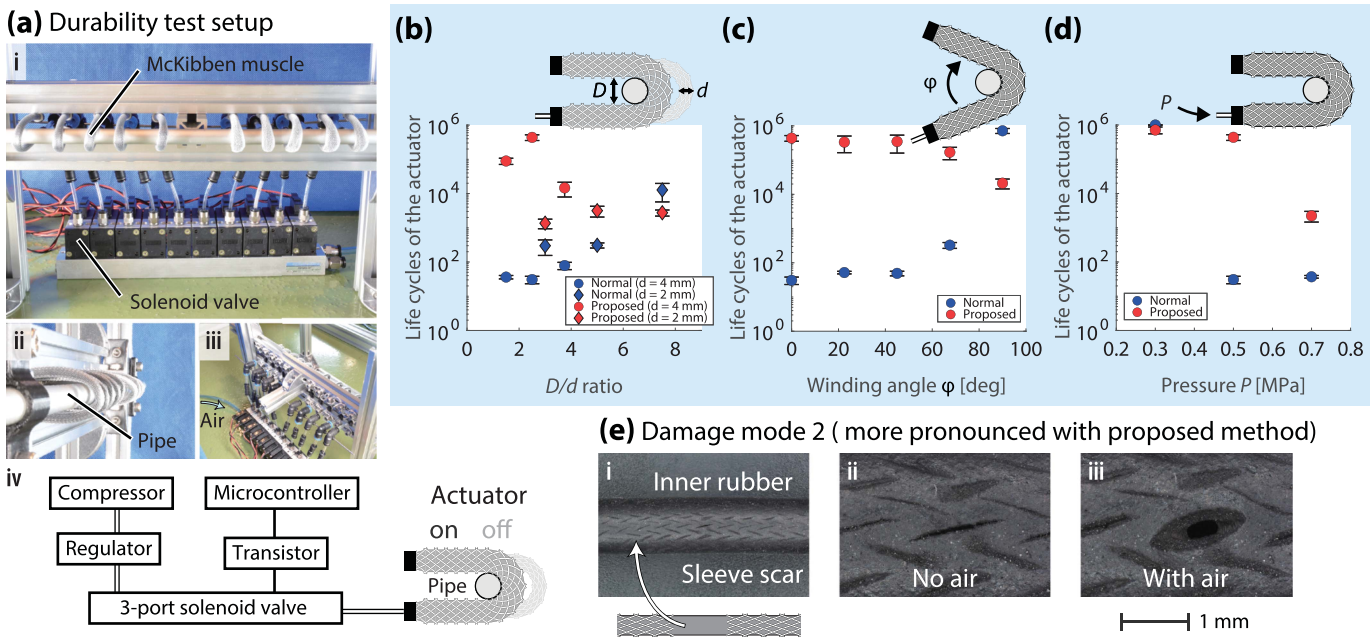

Fig. 5. (a) Durability test equipment and driving system. (b) Life cycles of the actuator with respect to D/d. (c) Life cycles of the actuator with respect to the thin McKibben muscle's angle φ. (d) Life cycles of the actuator with respect to the pneumatic pressure applied to the artificial muscle. (e) Surface of the inner rubber tube damaged by Damage Mode 2. Proposed method's adhesive increases rubber tube damage, enhancing Damage mode 2. Depending on parameters, this may reduce durability compared to conventional methods in Figs. b, c, and d.

0.3 MPa (Fig. 5(d)), normal artificial muscles endured a greater number of repeated cycles of operation than those using the proposed method. This indicates that sleeves with applied adhesive may be more prone to damaging the rubber tube than conventional sleeves. The sleeve marks are likely to be due to the high operating pressure of 0.5 MPa or 0.7 MPa, the small fiber diameter of the sleeve (0.16 mm), and the tiny protrusions of the adhesive. In fact, Fig. 5(d) shows that the number of cycles before Damage mode 2 failure is smaller when higher pressure is applied. Therefore, resolving this issue may involve reducing the operating pressure to the rated 0.3 MPa, increasing the sleeve fiber diameter, or smoothing the surface of fiber. The proposed method showed maximum durability improvement of 14,000 times at $D/d = 2.5$.

IV. Application of Thin McKibben Muscles Using the Proposed Method to Artificial Muscle-Driven Soft Tensegrity Robots

A. Single Module Durability Test

A tensegrity module [15], [16] was fabricated using the proposed artificial muscles. Twelve artificial muscles were used in this module. One artificial muscle is attached around the triangle which consists one strut and two rubber threads. Please see [16] for more details. Although, the structure which artificial muscle is attached is not a pipe, the D/d ratio is estimated in the scope of 0.5 to 2.5, and the angle is around 10 deg. Here, we investigate the durability of the tensegrity module under cyclic bending deformation (Fig. 6(a)). The adhesive is applied to all parts of the muscle.

A pneumatic pressure of 0.5 MPa was simultaneously applied to the 6 of 12 artificial muscles. The pressure was turned on for 2 s and off for 2 s because of the time required for exhaustion. In the case of the normal artificial muscles, one artificial muscle was damaged by Damage Mode 1 after approximately 100 repetitive movements. However, the artificial muscles with improved durability could withstand more than 50,000 repetitive movements, and one artificial muscle was damaged by Damage Mode 2.

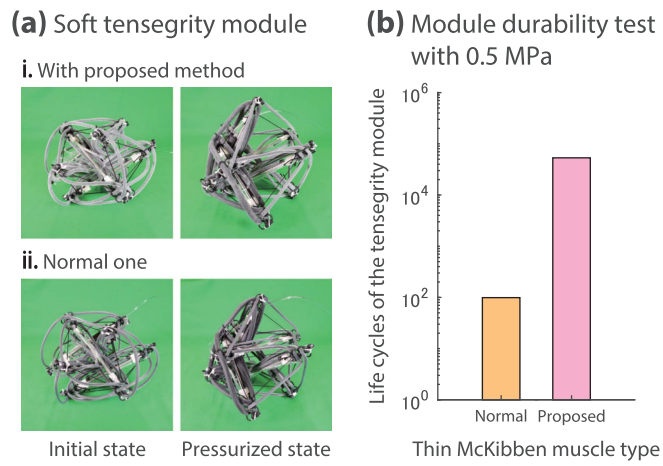

Fig. 6. (a) Bending deformation of soft tensegrity modules with and without the adhesive. (b) Durability test results of one tensegrity module.

B. Tensegrity Arm Durability Test

A soft tensegrity robot arm, as shown in Fig. 7(a) [15], was fabricated using the modules. In [15], although the applied

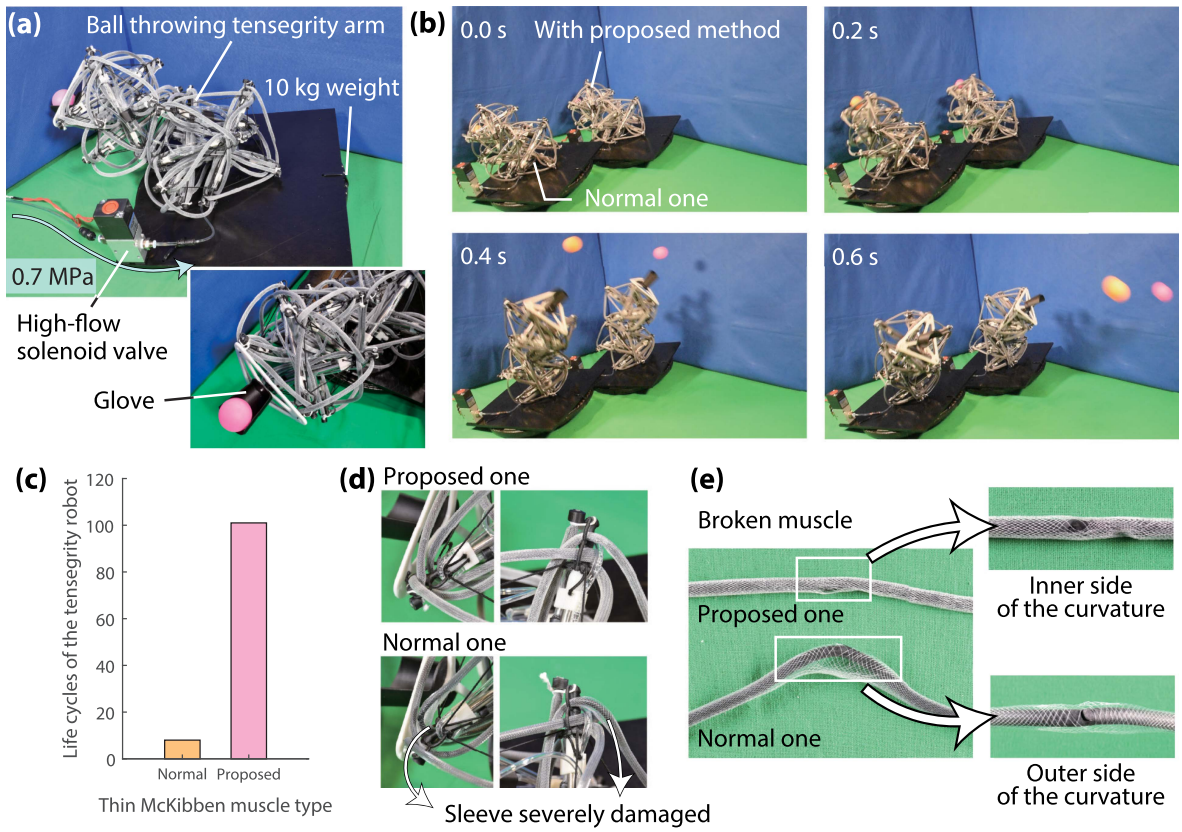

Fig. 7. (a) Ball-throwing tensegrity arm driven by thin pneumatic artificial muscles. (b) Ball-throwing experiment for two types of arms. One is with thin McKibben muscles using the proposed method; the other is with normal thin McKibben muscles. (c) Number of repetitions before breaking one artificial muscle for both types of arms. (d) Appearance of the artificial muscle sleeve after repetitive throwing experiment. (e) Appearance of the broken artificial muscle.

pressure was 0.4 MPa and the operation was static, repeated movements caused damage to the artificial muscles owing to sleeve deformation. The present study demonstrates that the proposed improvement in durability is expected to contribute to enhanced durability even during more dynamic movements.

In the artificial muscles attached to the tensegrity arm shown in Fig. 7(a). A high-flow solenoid valve (200E1, KOGANEI) was used to handle large flow rates. To prevent constriction of flow, the effective cross-sectional area of tubes and connectors was maintained at more than 3 mm^2. To perform dynamic movements, the tensegrity arm was mounted on a 10 kg weight. In addition, a glove made using a 3D printer was attached to the arm's end to enable throwing actions.

The throwing experiment is depicted in Fig. 7(b). The tensegrity arm could perform rapid movements using a high pressure of 0.7 MPa and a large flow rate without any constriction. The ball's distance was approximately 1000 mm for the arm with normal artificial muscles and approximately 800 mm for the arm with the proposed artificial muscles. These data are average values of five data sets. This difference in throwing distance was attributed to differences in contraction speed and friction caused by the adhesive. As shown in Fig. 4(f) and (g), there is a slight difference in the time constant of the contraction ratio. Additionally, the adhesive applied to the sleeve, as illustrated in Fig. 3, may increase the friction force between the sleeve and the tensegrity's attachment point.

Through repeated harsh throwing conditions, when using normal artificial muscles, the muscle broke after eight throws, whereas when using artificial muscles with the proposed method, it could withstand 101 throws (Fig. 7(c)). The durability of the thin artificial muscle under very severe conditions was thus improved by a factor of 12.7. The condition of the artificial muscle after the experiment is shown in Fig. 7(d). The actual state of the broken artificial muscle is depicted in Fig. 7(e). The normal artificial muscle broke on the outer side of the curvature, as shown in Fig. 2(c), while the artificial muscle using the proposed method broke on the inner side of the curvature. This indicates that under the application of a pressure of 0.7 MPa and the additional factor of the thin diameter of the rod wrapped around it (Fig. 2(a)), the internal adhesive may have peeled off owing to repeated impacts on the artificial muscle. However, there was only minimal damage to the sleeve even under this severe condition, and the improvement in the durability of the actuator was verified.

V. Conclusion

This study considered the improvement in durability under the repeated driving of thin artificial muscles in a bent state. First, the causes of damage while driving thin artificial muscles in a bent state were identified. Subsequently, a new method was proposed to enhance durability by applying adhesive to the sleeve to make a partition for preventing the misalignment of the fibers. This approach achieved thin artificial muscles with durability exceeding normal ones by over 10,000 times while maintaining contraction ratios and flexibility similar to conventional thin artificial muscles in the maximum case.

Moreover, this study focused on the application of the realized highly durable artificial muscles to a tensegrity robot. A tensegrity module with artificial muscles obtained using the proposed method and normal one were fabricated, and durability tests were conducted. When 0.5 MPa was repeatedly applied, it was confirmed that the proposed method enhanced module durability by more than 500 times. The modules were then used for a tensegrity robotic arm, and throwing motions were performed by applying 0.7 MPa. The robot with artificial muscles fabricated using proposed method showed a durability that was 12.7-times higher than that of conventional tensegrity robots in dynamic throwing motions. Furthermore, even in cases of damage, the method demonstrated minimal harm.

This research can be applied to effective applications such as fabric-like actuators that utilize artificial muscles in a bent state, support suits that employ these actuators, and high-contraction actuators created by interweaving artificial muscles. Furthermore, the ability to use artificial muscles in a bent state enhances the design freedom of robots. Therefore, the use of thin artificial muscles with high durability even under bending conditions is expected to have potential application in a wide range of robots in the future, and the findings of this study contribute to the advancement of soft mechatronics in the practical use.

ACKNOWLEDGMENT

The authors would like to thank Hiroto Kodama for his assistance with a part of the experiment.

REFERENCES

[1] C. Majidi, "Soft robotics: A perspective—current trends and prospects for the future," *Soft robot*, vol. 1, no. 1, pp. 5–11, 2014.

[2] H. F. Schulte, "The characteristics of the Mckibben artificial muscle," *Appl. External Power Prosthetics Orthotics*, vol. 874, pp. 94–115, 1961.

[3] B. Tondu and P. Lopez, "Modeling and control of McKibben artificial muscle robot actuators," *IEEE Control Syst. Mag.*, vol. 20, no. 2, pp. 15–38, Apr. 2000.

[4] R. M. Robinson, C. S. Kothera, R. M. Sanner, and N. M. Wereley, "Nonlinear control of robotic manipulators driven by pneumatic artificial muscles," *IEEE/ASME Trans. Mechatron.*, vol. 21, no. 1, pp. 55–68, Feb. 2016.

[5] R. M. Robinson, C. S. Kothera, and N. M. Wereley, "Variable recruitment testing of pneumatic artificial muscles for robotic manipulators," *IEEE/ASME Trans. Mechatron.*, vol. 20, no. 4, pp. 1642–1652, Aug. 2015.

[6] N. Delson, T. Hanak, K. Loewke, and D. N. Miller, "Modeling and implementation of Mckibben actuators for a hopping robot," in *Proc. IEEE 12th Int. Conf. Adv. Robot.*, 2005, pp. 833–840.

[7] S. Wakimoto, K. Suzumori, and J. Takeda, "Flexible artificial muscle by bundle of McKibben fiber actuators," in *2011 IEEE/ASME Int. Conf. Adv. Intell. Mechatron.*, 2011, pp. 457–462.

[8] G. Maloisel, E. Knoop, C. Schumacher, and M. Bächer, "Automated routing of muscle fibers for soft robots," *IEEE Trans. Robot.*, vol. 37, no. 3, pp. 996–1008, Jun. 2021.

[9] N. Takahashi, H. Takahashi, and H. Koike, "Soft exoskeleton glove enabling force feedback for human-like finger posture control with 20 degrees of freedom," in *2019 IEEE World Haptics Conf.*, 2019, pp. 217–222.

[10] K. Barhydt and H. H. Asada, "A high-strength, highly-flexible robotic strap for harnessing, lifting, and transferring humans," *IEEE Robot. Automat. Lett.*, vol. 8, no. 4, pp. 2110–2117, Apr. 2023.

[11] T. Hiramitsu, K. Suzumori, H. Nabae, and G. Endo, "Experimental evaluation of textile mechanisms made of artificial muscles," in *2019 2nd IEEE Int. Conf. Soft Robot.*, 2019, pp. 1–6.

[12] T. Abe et al., "Fabrication of "18 weave" muscles and their application to soft power support suit for upper limbs using thin Mckibben muscle," *IEEE Robot. Automat. Lett.*, vol. 4, no. 3, pp. 2532–2538, Jul. 2019.

[13] Y. Funabora, "Prototype of a fabric actuator with multiple thin artificial muscles for wearable assistive devices," in *2017 IEEE/SICE Int. Symp. Syst. Integration*, 2017, pp. 356–361.

[14] Y. Funabora, "Flexible fabric actuator realizing 3D movements like human body surface for wearable devices," in *2018 IEEE/RSJ Int. Conf. Intell. Robots Syst.*, 2018, pp. 6992–6997.

[15] R. Kobayashi, H. Nabae, and K. Suzumori, "Active-bending six-bar tensegrity modular robot driven by thin artificial muscles," *IEEE Robot. Automat. Lett.*, vol. 8, no. 11, pp. 7400–7407, Nov. 2023.

[16] R. Kobayashi, H. Nabae, G. Endo, and K. Suzumori, "Soft tensegrity robot driven by thin artificial muscles for the exploration of unknown spatial configurations," *IEEE Robot. Automat. Lett.*, vol. 7, no. 2, pp. 5349–5356, Apr. 2022.

[17] R. Kobayashi, H. Nabae, and K. Suzumori, "Large torsion thin artificial muscles tensegrity structure for twist manipulation," *IEEE Robot. Automat. Lett.*, vol. 8, no. 3, pp. 1207–1214, Mar. 2023.

[18] S. Lu et al., "6N-DoF pose tracking for tensegrity robots," in *Proc. Int. Symp. Robot. Res.*, 2022, pp. 136–152.

[19] A. P. Sabelhaus et al., "System design and locomotion of SUPERball, an untethered tensegrity robot," in *2015 IEEE Int. Conf. Robot. Automat.*, 2015, pp. 2867–2873.

[20] S. Spiegel, J. Sun, and J. Zhao, "A shape-changing wheeling and jumping robot using tensegrity wheels and bistable mechanism," *IEEE/ASME Trans. Mechatron.*, vol. 28, no. 4, pp. 2073–2082, Aug. 2023.

[21] Y. Koizumi, M. Shibata, and S. Hirai, "Rolling tensegrity driven by pneumatic soft actuators," in *2012 IEEE Int. Conf. Robot. Automat.*, 2012, pp. 1988–1993.

[22] C. Tawk, G. M. Spinks, M. in het Panhuis, and G. Alici, "3D printable linear soft vacuum actuators: Their modeling, performance quantification and application in soft robotic systems," *IEEE/ASME Trans. Mechatron.*, vol. 24, no. 5, pp. 2118–2129, Oct. 2019.

[23] G. Na, H. Nabae, and K. Suzumori, "Braided thin mckibben muscles for musculoskeletal robots," *Sensors Actuators A: Phys.*, vol. 357, 2023, Art. no. 114381.

[24] K. Suzumori, S. Seita, and S. Wakimoto, "Mckibben artificial muscle," 2016, Japan Patent JP 2016-173117A.

[25] B. Tondu, "Modelling of the Mckibben artificial muscle: A review," *J. Intell. Mater. Syst. Struct.*, vol. 23, no. 3, pp. 225–253, 2012, doi: 10.1177/1045389X11435435.